Simulating and Measuring Otoacoustic Emissions

Cecilia Casarini

A final project dissertation submitted in partial fulfilment
of the requirements for the degree of

Master of Science (MSc)

Acoustics and Music Technology

Acoustics and Audio Group
Edinburgh College of Art
University *of* Edinburgh

August 2016

Supervisor: Dr Michael Newton

Abstract

Otoacoustic emissions(OAEs) are low-level sounds generated in the inner ear either spontaneously or by an evoking stimulus. OAEs have been used for years in hearing research to test our understanding of the auditory system; moreover they are already employed in newborn hearing screenings and it has been suggested that they could become a biometric instrument in the future. This dissertation describes the work I have done during the final project of the Acoustics and Music Technology MSc at the University of Edinburgh. The project is divided in two parts: in the first one a physical model of the cochlea is implemented in Matlab, while in the second part the OAEs are measured through a specific equipment and analysed. The model and the experiments are eventually compared, to understand where and how the implementation can be improved. The model, inspired by A. Moleti formulation [1], proved to be reliable and accurate in both its linear and nonlinear implementations and the emissions have been successfully simulated. A potential extension could involve the simulation of SOAEs and a clearer distinction of the way the emissions are generated (whether by a linear reflection or a nonlinear distortion). The measurements successfully recorded DPOAEs and TEOAEs, even if a better analysis technique is needed for the transient emissions. Finally the measurement of DPOAEs near the hearing threshold has suggested a possible future research on the advantages of substituting audiograms with OAEs screenings.

Declaration

I do hereby declare that this dissertation was composed by myself and that the work described within is my own, except where explicitly stated otherwise.

Cecilia Casarini
August 2016

Acknowledgements

Contents

List of Figures

Chapter 1

Introduction

Otoacoustic emissions (OAEs) are low-level sounds that are generated in the inner ear either spontaneously or as a reaction to an evoking stimulus and that can be recorded in the ear canal. These emissions represent a fascinating phenomenon that has been studied for ears to test our understanding of the human auditory system. Furthermore OAEs are already used in some countries for newborn hearing screenings and it has been suggested that in the future they could serve as a biometric instrument for recognition. My final project is part of the MSc in Acoustics and Music Technology at the University of Edinburgh and consisted in coding with Matlab a physical model of the cochlea able to simulate OAEs and then recording the emissions in the lab. The lab measurements have been obtained by using a probe containing a microphone and two speakers and by implementing a Labview code connected to the probe through a NI hardware. This work was supported by several readings on the specific subject of OAEs and on hearing research in general, as can be seen in the bibliography at the end of the dissertation.
In Chapter 2 I introduce the topic of hearing research by highlighting the most important physiological and physical features of the human auditory system. In particular the outer, middle and inner ear are described together with the three phases of the transduction of sound from pressure wave to electrochemical signal.
The phenomenon of otoacoustic emissions is described in Chapter 3, where the two main classifications of the emissions are explained in detail.
In Chapter 4 the three most relevant (for this dissertation) physical models of the cochlea are described; in particular the model of Moleti, that is at the base of the project and that can be found in [1], is explained and analysed.
Chapters 5 and 6 present the results obtained respectively by simulating and measuring otoacoustic emissions. The simulations have been obtained by implementing the model of Moleti in Matlab and they show the properties of the model, in particular its nonlinear and saturating active mechanism and the generation of DPOAEs and TOAEs. The measurements have been obtained in the anechoic chamber using a specific probe, a NI hardware and a Labview code.

Finally, the conclusions on the results accomplished during this final project and further ideas for future research on the subject are presented in Chapter 7.
Many mechanisms at the base of human hearing are still unknown and research is needed in this field not only to better understand the human nature, but also to apply our knowledge to technology and engineering, for example to improve cochlear implants, headphones and in general our auditory experience. Therefore, otoacoustic emissions are a topic worth investigating and I hope that this work will represent a good and valid starting point for me in order to join the hearing research community after the MSc and to achieve a solid knowledge of this fascinating topic.

Chapter 2

Physiology of the Ear

The study of the physiology and physics of the ear is the first step that one needs to tackle in order to build a physical model of the cochlea. In this chapter I will summarise the most important physical and physiological features of the outer, middle and inner ear. This is not intended to be an extensive description of the hearing auditory system, but simply an introduction that can help the reader to familiarise with the main topics at the base of the dissertation and with the most important features that will be found in the physical model. The human ear is a transducer that converts mechanical energy into electrochemical signals transmitted to the brain; this transduction is divided in three phases, as described in the next sections. Before describing these phases it is important to introduce briefly the concepts of impedance and nonlinearity.
We can define the impedance as the ratio between the pressure of sound and its velocity in a medium: $z = p/v$. The impedance of an infinite medium for plane waves is a specific characteristic of the medium itself and it is measured in units of $(\mathrm{N/m^2})/(\mathrm{m/sec})$. The impedance of the fluid in the inner ear is much higher than that of the air in the ear canal, therefore in the three phases of the transduction (above all in the middle ear) a pressure gain is applied in order to match the two different values of the impedance and hence to avoid the reflection of the incoming sound wave.
Generally speaking a nonlinear system identifies a system in which the output is not directly proportional to the input: if the input is changed by a factor k, the output will not be changed by the same factor [2]. Furthermore, while in a linear system the output contains the same frequencies of the input, in a nonlinear system the output may also contain harmonics and linear combinations of the input frequencies [2].

2.1 Outer Ear

The outer ear is the visible part of the auditory system. It is composed of the pinna, which includes the concha, the ear canal, that extends from the pinna to the eardrum,

and the tympanic membrane (or eardrum), a membrane 0.1 mm thick that vibrates whenever a sound pressure wave enters the ear canal. Its main functions are sound localization, through the pinna and the concha, and pressure amplification performed by the resonances of the ear canal.

The position of the source and the differences in timing and intensity of the sound waves striking the left and the right ear are undoubtedly important for sound localization. In addition to this information, the raised ridges of the concha and the pinna help us to distinguish the directionality of the sounds by reflecting the pressure waves into the ear canal in different ways, depending on the position of the source in relation to that of the ear itself.

We can think about the ear canal as a tube closed at one extremity; therefore its resonant frequencies are given by the formula: $f_n = (2n-1)\frac{c_s}{l}$, where c_s is the speed of sound, around 340 m/sec and l is the length of the ear canal, on average 2.5 cm. Hence, in particular, $f_1 = 3400$ Hz. These resonances do not just increase the pressure of waves that have corresponding frequencies, but they have a complementary effect on all the waves in the frequency range 2000 to 7000 Hz [2].

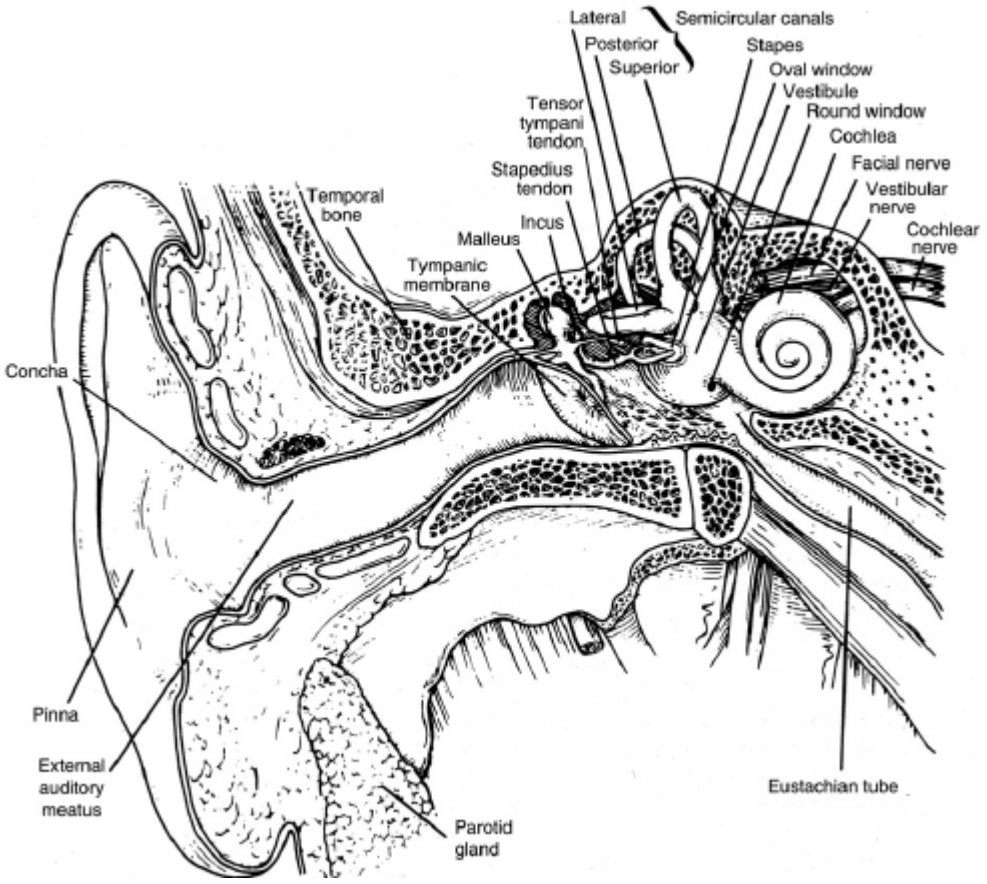

Figure 2.1: External, middle and inner human ears [2].

2.2 Middle Ear

The middle ear is a cavity full of air. The air pressure is transmitted through the three tiny bones known as the ossicles: the malleus, the incus and the stapes. These tiny bones act as acoustic impedance transformers between the ear canal and the fluid in the cochlea: without this impedance matching mechanism the sound wave would be totally reflected, as the impedance of the fluid is much higher than that of the air.
This impedance matching is performed by applying two gains to the incoming pressure wave. Since the area of the tympanic membrane is bigger than the stapes footplate, a first gain is given by the ratio between the two areas: $\frac{A_{eardrum}}{A_{stapes}} = \frac{60}{3.2} = 18.75$. Furthermore, the lever mechanism and the geometry of the three bones apply a second gain: by decreasing the velocity of the pressure wave and increasing its amplitude, they apply an additional gain of 4.4, so that the total gain becomes $18.75 \times 4.4 = 82.5$. The transfer function of the outer ear can be seen as a filter centred at 1000 Hz, as shown in figure 2.3. This mechanism is most efficient in the range around 1-2 kHz, above this frequency the transmission is reduced. This transmission is also reduced at low frequencies, as the middle ear muscles perform a sort of gain control in order to protect the ear from noise damage and to reduce the masking of high frequencies [2].

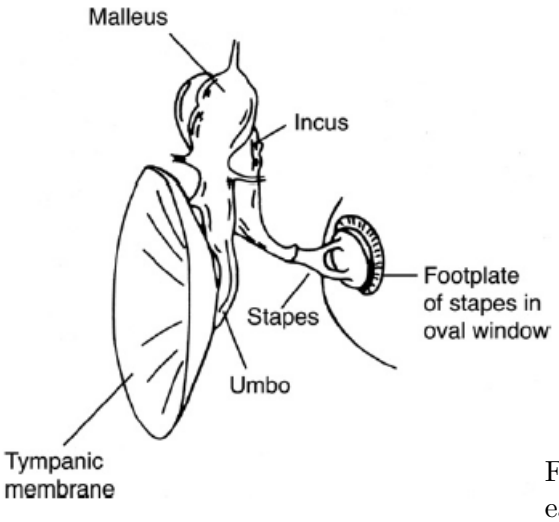

Figure 2.2: Middle ear ossicles [2].

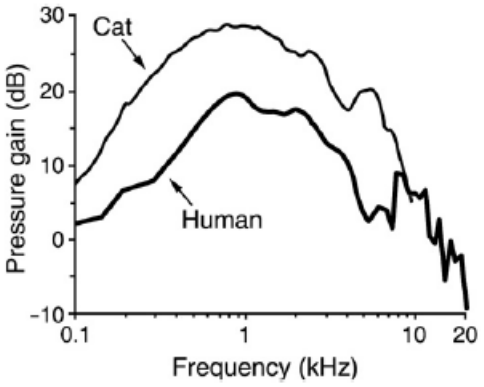

Figure 2.3: Transfer function of the middle ear [2].

2.3 Inner Ear

The inner ear is the actual place where the transduction of sound into electrochemical signals is performed. The cochlea is a spiral-shaped cavity 33 to 35 mm long that acts as a Fourier analyser that separates frequency information for the brain. As illustrated in Figure 2.4, the cochlea is divided by a inner membraneous partition into three fluid

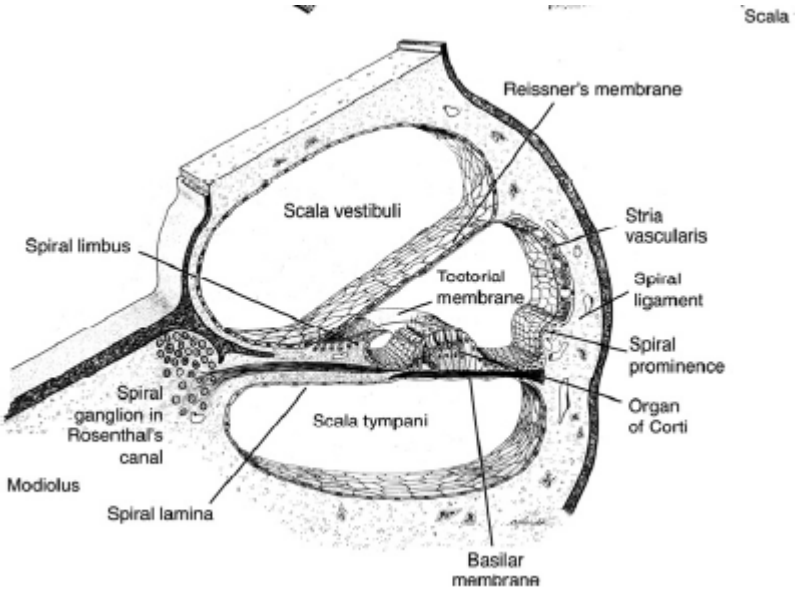

Figure 2.4: Inner ear [2].

filled spaces: the scala vestibuli, the scala media and the scala tympani (In the physical model described in Chapter 4 just the two outer scalae are taken into account). This information is particularly important for the purpose of this dissertation, as the input of one of the main functions of the physical model of the cochlea is the pressure difference (p_d) between these fluids.

The first important function of the cochlea is that of tonotopy. The pressure wave coming from the middle ear generates a movement in the fluid and consequently the basilar membrane vibrates, generating a travelling wave that reaches a peak of amplitude when the local impedance (that changes because of different stiffness) is minimized. Higher input frequencies correspond to peaks in the basal region, closer to the middle ear and to the oval window and lower frequencies have their peak in the apical region, closer to the round window and further away from the middle ear. If we imagine to uncoil the cochlea and the basilar membrane, it can be seen that equal distances along the basilar membrane correspond to a fixed interval, in other words the distance between the resonant peak of two octaves will always be the same (like in the piano!)

The other important function of the cochlea is the active compressive feedback. Above the basilar membrane there is the Organ of Corti, a sensory epithelium containing auditory transducers, namely the outer hair cells and the inner hair cells; the hair cells contain many hairs, called stereocilia. The vibration of the basilar membrane results in the contraction of the outer hair cells, that transmit neural signals to the brainstem. Then, the brainstem in turn transmits an electrical signal to the outer hair cells again, and this signal amplifies the vibration of the basilar membrane. This active feedback

process is compressive, allowing the wide human hearing range that goes from 0 to 120 dB. Finally the vibration of the amplified basilar membrane results in the contraction of the inner hair cells that transmit an electrical signal to the acoustical nerve and eventually to the corresponding tonotopic region in the cerebral cortex [6], [7].

Chapter 3

Otoacoustic Emissions

Otoacoustic emissions have been known and studied since the late 1970s. The existence of spontaneous sounds generated by the active cochlea had been predicted by the astronomer T. Gold in 1948 [8] and was then confirmed by D. T. Kemp in 1979 [9], who experimentally measured the spontaneous emissions (SOAEs) and discovered that they could also be evoked by a transient sound. These emissions do not seem to have a direct role in hearing, however stimulus-evoked OAEs can be generated in all the healthy cochleas. Understanding this phenomenon is a challenging goal, as it includes the analysis of the full signal, from the acoustics of the outer ear where the evoking stimulus is originated, passing through the mechanics of the middle ear (that works well in both directions) and finally reaching the inner ear, where the emission is originated. Eventually the pressure wave recorded in the ear canal is the sum of the ringing stimulus and the otoacoustic emission, that have to be separated in order to be analysed.
OAEs have an important role in hearing research, as they are considered to be a by-product of the cochlear amplifier and of its nonlinearity. For this reason they are a useful mean of investigation of the inner ear and in general they have been used since 1978 as a proof of the active processes in the cochlea. Outside research, OAEs have been also used for many years for clinical purposes, above all in the hearing screening tests for newborns, since the absence of some of these emissions is strictly correlated to hearing impairment [10],[11]. Moreover, it has been suggested that the uniqueness of DPOAEs could lead to their use as a biometric recognition instrument in the future [12], [13].
There are two main ways of classifying OAEs: the first is used in clinical applications and it is based on the type of evoking stimulus used, while the second is more popular for research purposes and it is based on the generation mechanism within the cochlea.

3.1 Stimulus-based Classification

According to the stimulus-based classification of OAEs, they can be divided in: spontaneous (SOAEs), transient evoked (TEOAEs), stimulus-frequency (SFOAEs) and distortion product (DPOAEs).

3.1.1 SOAEs - Spontaneous Otoacoustic Emissions

SOAEs can be detected in the ear canal without using an evoking stimulus, since they are a by-product of the physiological noise of the inner ear and a consequence of its active nonlinear processes. As shown in Figure 3.1 [3], spontaneous otoacoustic emissions are weak narrowband signals and can have a variable amplitude, generally lower than 5 dB SPL and they are present in the 40-60% of the population. SOAEs are generally measured in the frequency domain, by using long-term spectral averaging. Even if in general they cannot be detected in subjects with hearing impairment, their absence does not imply any audiological problems.

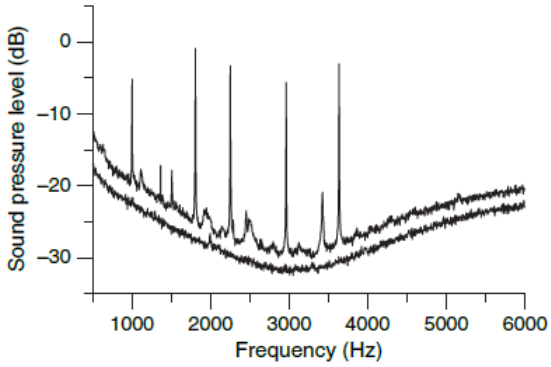

Figure 3.1: Spectrum of SOAEs measured from two subject without hearing impairment [3]. The first subject emits 11 emissions, while in the second subject (shifted by 2 dB for visualization purposes) no emissions are present.

3.1.2 TEOAEs - Transient Evoked Otoacoustic Emissions

TEOAEs are usually evoked by a transient stimulus, as a click, a tone burst, or a chirp. Using a short transient sound to evoke the emission has revealed to be an efficient way of approaching a common problem related to the analysis of OAEs: the signal recorded in the ear canal is the sum of the stimulus and the emission and a short click can be easily separated from the OAE because of the time delay between the two. Despite the time delay though, the first part of the emission could be hidden by the ringing stimulus and the overlap is even more present for high level stimuli. Therefore the preferred stimuli correspond to lower frequencies, since the input has to cover a longer

path towards the apical region of the cochlea before travelling back to the middle and outer ear, and this results in a longer delay and a clearer distinction between the OAE and the stimulus.

3.1.3 SFOAEs - Stimulus Frequency Otoacoustic Emissions

SFOAEs are low level emissions generated by the cochlea at the frequency of the evoking continuous pure tone stimulus. TEOAEs and SFOAEs are often grouped together, because they are both at the same frequency of the evoking stimulus (in the first case a transient sound and in the second case a pure tone) [4]. Like TEOAEs they are present in the 98% of population with healthy hearing system and they are generated by the same mechanisms. Having the same frequency and a lower level than the stimulus, SFOAEs are difficult to measure and analyse. Kemp D. T. and Chum R. introduced a method [14] to study these emissions that takes advantage of the fact that, at high levels, the stimulus dominates the response in the ear canal. By measuring the signal at 70dB, when it is mainly composed by the stimulus (as shown in Figure 3.2), it is possible to predict the portion of the signal at lower levels corresponding to the stimulus and therefore the otoacoustic emission is calculated. Another method alternates as input the stimulus and a higher level signal composed by the stimulus summed to a second tone with a slightly higher frequency, that suppresses the emission. Subtracting the second measured pressure, that contains the stimulus and the second tone, to the first one, composed by the emission and the stimulus, it is possible to obtain the emission and the second tone together, that can be easily distinguished because of their different frequencies.

3.1.4 DPOAEs - Distortion Product Otoacoustic Emissions

DPOAEs are evoked by a stimulus composed by a pair of tones $f_1 < f_2$ with a frequency ratio $f_2/f_1 < 1.4$ (usually 1.22 is chosen). The nonlinearity of the cochlea produces intermodulation and harmonic distortion, therefore the emission contains tones at the two stimulus frequencies but also at linear combinations of f_1 and f_2, the most commonly measured being $f_{dp} = 2f_1 – f_2$. Figure 3.3 shows an example of DPOAEs measured from chinchillas [3]. As explained below DPOAEs are considered to be a mix of two different generation processes within the cochlea (a coherent reflection from the f_{dp} place and a non-linear distortion from the f_2 place), the contribution of each process depending on the parameters of the stimulus.

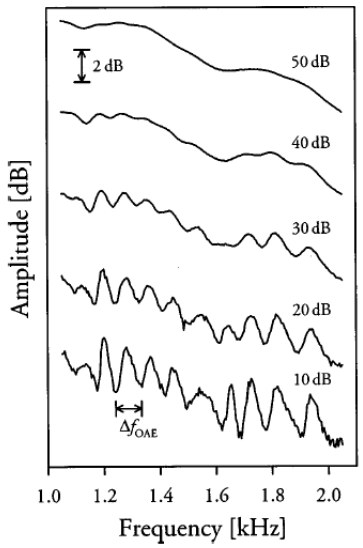

Figure 3.2: SFOAEs at different amplitude levels [4]. The higher level pressure waves are dominated by the stimulus, while in the lower level waves the emissions can be clearly seen.

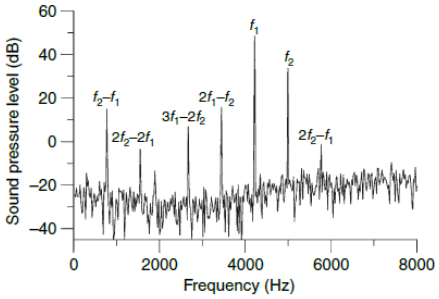

Figure 3.3: DPOAEs measure from a chinchilla [3].

3.2 Generation-based Classification

The second classification method distinguishes OAEs according to the way they are generated within the inner ear. Until 1999 all evoked OAEs were considered to be a by-product of the same mechanism, namely a nonlinearity at the peak of the travelling wave, responsible for backscattering the incoming signal to the ear canal [15]. Shera A. and Guinan J. J. [4] elaborated a generation-based taxonomy, dividing the emissions in linear reflection and nonlinear distortion products, as can be seen in Figure 3.4. This classification was inspired by an idea proposed by Kemp and Brown in 1983 [16] that distinguished the emissions respectively in "place fixed" and "wave fixed". It is important to notice that evoked emissions can be generated by a mix of both mechanisms; in particular, low level SFOAEs and TEOAEs are thought to be generated by linear reflection and DPOAEs (when the reflection from f_{dp} can be neglected) by nonlinear distortion. Mid and high level SFOAEs and TEOAEs are thought to be generated by linear reflection as well, and their nonlinear growing with level is explained by a later amplification by the outer hair cells, that is not responsible for their generation. Despite this, a small part of their energy could be caused by a nonlinear distortion, as well as DPOAEs are sometimes a mixture of the two mechanisms. Therefore it is not possible to elaborate a fixed correspondence between the two classifications [4], [17].

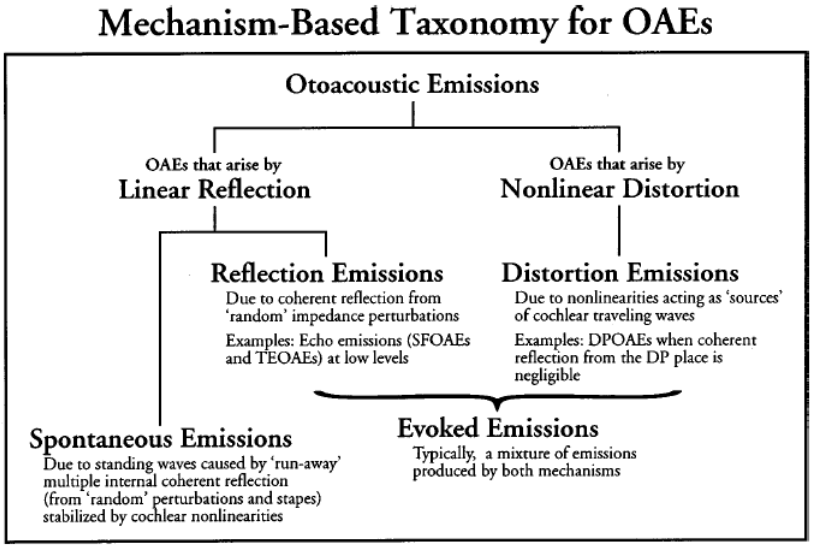

Figure 3.4: Taxonomy for mammal otoacoustic emissions proposed by Shera [4].

3.2.1 Linear Reflection

Linear reflection emissions are thaught to be the result of random distributed micro-irregularities in the basilar membrane that scatter back the incoming stimulus. Since the amplitude of the stimulus has a peak at the resonance place, there will be a significant reflection only when the irregularity is next to it, while waves reflected in other regions of the basilar membrane will cancel out before reaching the stapes. These pre-existing perturbations in the mechanics are fixed, therefore a small change in frequency will not change the position from which the reflection originates; this is why this kind of emissions are also called "place fixed". Low level TEOAEs and SFOAEs are originated by linear reflection and they are characterised by a slow varying amplitude that grows linearly with the stimulus and by a rapidly rotating phase [18].

3.2.2 Nonlinear Distortion

The active nonlinear action of the outer hair cells, pushing and pulling on the basilar membrane, is considered to be responsible for the generation of nonlinear emissions: during the amplification process a part of the energy added to the basilar membrane vibration "escapes" and creates a backward-travelling wave. This mechanism causes a distortion of the incoming travelling wave that will contain linear combinations of the frequencies corresponding to that particular tonotopic region. A change in the stimulus frequency will change also the position from which the distortion originates; hence, this kind of OAEs are also called "wave fixed". OAEs with a mainly frequency-independent phase are considered to be generated by non-linear distortion [4].

Chapter 4

Cochlear Models

Implementing physical models of the cochlea, or more in general of the ear, and comparing the resulting simulations with experimental data, allows us to verify our understanding of the mechanical and physical characteristics of the human auditory system.
Before Kemp's discovery of otoacoustic emissions (OAEs) in 1979, physical models of the ear were passive and mostly based on Von Békésy's measurements of dead cochleas [19]. The proof of OAEs existence marked the beginning of new *in vivo* experiments and gave birth to a new generation of cochlear models that included nonlinearities and active processes in their formulation [20].
Today many different models can be found in the literature, each of them being of course an oversimplification of the complexities of the human auditory system. The goal of this research is to measure OAEs and compare the experimental data with a cochlear model that takes into account in its formulation the generation of these fascinating and important emissions. Therefore, I have chosen as a starting point for my research two specific models: the first is Neely and Kim model [5], which is a simple frequency-domain model that includes an active mechanism; the second is its modification as a state space formulation published by Elliott [21], that takes into account the generation of SOAEs.

4.1 The Neely and Kim Model

The Neely and Kim [5] model is a linear representation of a cat cochlea based on a frequency-domain formulation of a lumped-element system that also includes an active dynamic; in this chapter its adaptation to cochlear human parameters implemented by Ku [20] will be presented. One advantage of this model is that, despite its semplicity and linearity, it allows to predict the frequency response of every cochlear partition and the distribution of motion along the cochlea at a given frequency. As will be explained

in Chapter 5, this model represents a good starting point for a nonlinear formulation in the time domain.
The micro-mechanical model of the inner year is a two-deegrees-of-freedom-system, representing the dynamics of a radial slice of the cochlea. It is composed by two masses (m_1, m_2), corresponding to the tectorial and basilar membranes, three springs (k_1, k_2, k_3) and three dampers (c_1, c_2, c_3) that model the biological stiffness and mechanical characteristics of the inner ear and of the fluid surrounding it, as illustrated in Figure 4.1. The input to the system is the pressure difference p_d between the two

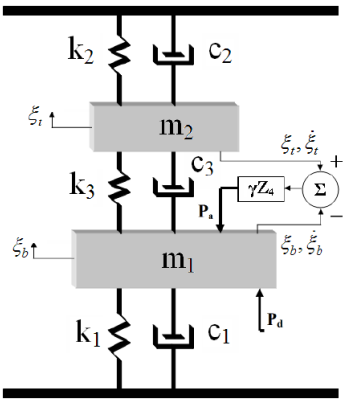

Figure 4.1: Lumped element of cochlea micromechanics as modelled by Neely and Kim [5].

fluid-filled cavities of the cochlea, while the output is the basilar membrane velocity. Being ξ_b the basilar membrane maximum displacement, it is useful to calculate the basilar membrane admittance, i.e. the ratio of output velocity to input pressure. As derived by Neely and Kim [5]:

$$\frac{\dot{\xi}_b(x)}{p_d(x)} = \frac{1}{g[Z_1(x) + Z_2(x)(\frac{Z_3(x)-\gamma Z_4(x)}{Z_2(x)+Z_3(x)})]} \tag{4.1}$$

where:

$$Z_1(x) = \frac{k_1(x)}{jw} + c_1(x) + jwm_1(x) \tag{4.2}$$

$$Z_2(x) = \frac{k_2(x)}{jw} + c_2(x) + jwm_2(x) \tag{4.3}$$

$$Z_3(x) = \frac{k_3(x)}{jw} + c_3(x) \tag{4.4}$$

$$Z_4(x) = \frac{k_4(x)}{jw} + c_4(x) \tag{4.5}$$

The values of the parameters c_1, c_2, c_3, c_4 and k_1, k_2, k_3, k_4 are the result of empirical experiments and physical knowledge and their retuned version compared to the original

model can be found in Ku [20]. g is the lever gain of the basilar membrane to the inner hair cells. Z_1, Z_2, Z_3, Z_4 represent respectively the mechanical impedance of the Organ of Corti, the mechanical impedance of the tectorial membrane, the coupling between the outer hair cells and the tectorial membrane and the impedance of the cochlear amplifier. γ is the feedback gain, with $\gamma = 0$ representing a passive system and $\gamma = 1$ the active response. The derivation of the above equations can be found in Ku [20].
The admittance of the tectorial membrane is the following:

$$\frac{\dot{\xi}_t(x)}{p_d(x)} = \frac{1 - [\frac{\dot{\xi}_b(x)}{p_d(x)}][gZ_1(x)]}{[Z_2(x) + \gamma Z_4(x)]} \tag{4.6}$$

As shown in Figure 4.1, the active element included in Neely and Kim passive model acts as a feedback loop on the passive system and it is represented by p_a, i.e. the pressure generated by the outer hair cells, defined as:

$$p_a(x) = -\gamma Z_4(x)\dot{\xi}_c(x) \tag{4.7}$$

where:

$$\dot{\xi}_c(x) = g\dot{\xi}_b(x) - \dot{\xi}_t(x) \tag{4.8}$$

The cochlear macromechanics are represented by Neely and Kim [5] as a series of independent oscillators, as described above, coupled through the fluid. The cochlea is modelled by a 1D box model, similar to the classical de Boer representation [22]. The pressure wave can be therefore represented by a one-dimension longitudinal wave equation derived in [23]:

$$\frac{\partial^2 p_d(x,\omega)}{\partial^2 x} - \frac{2j\omega\rho}{HZ_{cp}(x,\omega)} p_d(x,\omega) = 0 \tag{4.9}$$

where H is the height of the fluid chamber, ρ is the density of the cochlear fluid and Z_{cp} is the cochlear partition impedance, inverse of the admittance Y calculated below. The boundary conditions at the base of the cochlea and at the helicotrema are given by:

$$\frac{\partial p}{\partial x}\Big|_{x=0} = -2j\omega\rho u_{st} \tag{4.10}$$

and:

$$p_d\Big|_{x=L} = 0 \tag{4.11}$$

where u_{st} is the stapes velocity and L s the length of the cochlea.
We can now divide the length of the cochlea L in N elements, where $\frac{L}{N-1} = \Delta$ and use

a finite difference domain method to discretise Eqs. (4.9) to (4.11):

$$\frac{p_d(n+1) - 2p_d(n) + p_d(n-1)}{\Delta^2} - \frac{2j\omega\rho}{HZ_{cp}(n)}p_d(n) = 0 \tag{4.12}$$

$$\frac{p_d(2) - p_d(1)}{\Delta} = -2j\omega\rho u_{st} \tag{4.13}$$

$$p_d(N) = 0 \tag{4.14}$$

It is then possible to rewrite te cochlea wave equation and its boundary conditions in matrix form:

$$F = \frac{1}{\Delta^2}\begin{bmatrix} -\Delta & \Delta & & & 0 \\ 1 & -2 & 1 & & \\ & \ddots & \ddots & \ddots & \\ & & 1 & -2 & 1 \\ 0 & & & & \Delta^2 \end{bmatrix} \tag{4.15}$$

$$M = \frac{2j\omega\rho}{H}\begin{bmatrix} Y_m & & & & 0 \\ & Y_{cp}(2) & & & \\ & & \ddots & & \\ & & & Y_{cp}(N-1) & \\ 0 & & & & Y_H \end{bmatrix} \tag{4.16}$$

$$p_d = \begin{bmatrix} p_d(1) \\ \ddots \\ p_d(n) \\ \ddots \\ p_d(N) \end{bmatrix} \tag{4.17}$$

$$q = \begin{bmatrix} -2j\omega\rho u_{st} \\ 0 \\ \ddots \\ \ddots \\ 0 \end{bmatrix} \tag{4.18}$$

F and M are $N \times N$ matrices, p_d and q are $N \times 1$ matrices.
By obtaining the wave equation of the cochlea in matrix form it is possible to use a differential equation solver with Matlab and obtain the pressure difference p_d at every

location. Given an input frequency, the velocity of the basilar membrane at a certain position along the cochlea can be therefore obtained by:

$$\dot{\xi}_b(x,\omega) = \frac{p_d(x,\omega)}{Z_{cp}(x,\omega)} \tag{4.19}$$

4.2 The Elliott Model

The model of Elliott is a state-space formulation in time domain of the Neely and Kim discretised cochlear model. The state-space method is used to replace a n^{th}order differential equation with a first order matrix differential equation. The state of a dynamical system refers to a minimum set of variables, called state variables, that fully describe the system and its response at any time and for any given set of inputs. The state-space representation is given by:

$$\dot{z}(t) = Az(t) + Bu(t) \tag{4.20}$$

$$y(t) = Cz(t) + Du(t) \tag{4.21}$$

where:

$z(t)$ is the $(n \times 1)$ vector of the states (or states vector) of an n^{th}-order system,
A is the $(n \times n)$ states matrix, that contains the mechanics of the model,
B is the $(n \times r)$ input matrix that scales the r input(s) to the system,
C is the $(m \times n)$ output matrix,
D is the $(m \times r)$ transition matrix,
$u(t)$ is the $(r \times 1)$ input vector composed of the system input functions,
$y(t)$ is the $(m \times 1)$ output vector composed of the defined m outputs

The system has one input and one output and it has two degrees of freedom with two states associated with every mass; therefore, $n = 4$ (4^{th}order system), $r = 1$ and $m = 1$. The 4 state variables are chosen to represent the displacement and the velocity of the basilar membrane and the tectorial membrane:

$$\dot{\xi}_b(t) = z_1 \tag{4.22}$$

$$\xi_b(t) = z_2 \tag{4.23}$$

$$\dot{\xi}_t(t) = z_3 \tag{4.24}$$

$$\xi_b(t) = z_4 \tag{4.25}$$

$$\tag{4.26}$$

I will not describe in detail the model of Elliott, since similar passages are applied in the model of Moleti outlined in the following section. Nevertheless it is important to know that the model of Moleti is inspired by the state-space formulation of Elliott and in some sense it is a simplified version of it, as it is a one-degree-of-freedom system that includes one mass in its independent oscillators. The simplification applied by Moleti is important in order to reduce the overall complexity of the system and being able to generate the emissions. A too complex system would in fact result in a slower implementation. In the model of Elliott, after assigning the state space variables, the micromechanics and macromechanics of the systems are solved together by a matrix solver in Matlab (i.e. the ode45). This solution can be found in [21], [24] and [25] and the main ideas behind it will be explored in the next section, as they are also behind the model of Moleti.

4.3 The Moleti Model

The Moleti cochlear model is a state-space formulation based on the Elliott scheme and applied to a single-degree-of-freedom system, where the only moving mass represents the basilar membrane. All the parameters used in the equations of this section can be found in [1], [6] and in the Matlab code in Appendix A.
Moleti rewrites the cochlear wave equation and its boundary conditions in the following way:

$$\frac{\partial^2 p(x,0,t)}{\partial^2 x} = \frac{2\rho}{H}\ddot{\xi}(x,t) \tag{4.27}$$

$$\frac{\partial p(x,z,t)}{\partial z}\Big|_{z=0} = 2\rho\ddot{\xi}(x,t) \tag{4.28}$$

and:

$$\frac{\partial p(x,z,t)}{\partial z}\Big|_{z=H} = 0 \tag{4.29}$$

The first element of the N partitions of the model corresponds to the middle ear dynamics and is represented by:

$$\frac{\partial p}{\partial x}\Big|_{x=0} = 2\rho\ddot{\xi}_{ow} \tag{4.30}$$

where $\ddot{\xi}_{ow}$ represents the stapes acceleration and it is described by:

$$\ddot{\xi}_{ow}(t) + \gamma_{ow}(t)\dot{\xi}_{ow}(t) + \omega_{ow}^2\xi(t) = \frac{p(0,t) + G_{me}P_{dr}(t)}{\sigma_{ow}} \tag{4.31}$$

The last element of the N partitions represents the helicotrema, described by:

$$p(L, z, t) = 0 \tag{4.32}$$

Finally, all the elements from 2 to N-1 are given by the following equation:

$$\ddot{\xi}(x,t) + \gamma_{bm}(x, \xi, \dot{\xi})\dot{\xi}(x,t) + \omega_{bm}^2(x, \xi, \dot{\xi})\xi(x,t) = \frac{p(x,0,t)}{\sigma_{bm}} \tag{4.33}$$

where ω_{bm} and γ_{bm} are responsible for the frequency-place mapping described by the Greenwood equations:

$$\omega_{bm}(x) = \omega_0 e^{-k_w x} + \omega_1 \tag{4.34}$$

$$\gamma_{bm}(x) = \gamma_0 e^{-k_\Gamma x} + \gamma_1 \tag{4.35}$$

In the model of Moleti [1] the cochlea is assumed to be scale invariant; hence, the two Greenwood equations are modified in:

$$\omega_{bm}(x) = \omega_0 e^{-k_w x} \tag{4.36}$$

$$\gamma_{bm}(x) = \gamma_0 e^{-k_w x} \tag{4.37}$$

Therefore:

$$\frac{\omega_{bm}(x)}{\gamma_{bm}(x)} = Q \tag{4.38}$$

where Q is a constant representing the cochlear tuning.
We can now rewrite equation Eq. (4.27) in the semi-finite-difference-scheme as following:

$$FP(t) = \ddot{\Xi}(t) \tag{4.39}$$

where F is detailed in equation Eq. (4.15). Moleti then makes use of the state-space formulation and assigns to the $2N$ dimensional vector Z the variables of velocity $\dot{\xi}$ and displacement ξ:

$$Z_j = [\dot{\xi}_j(x_j, t), \xi_j(x_j, t)] \tag{4.40}$$

The equations Eqs. (4.30) to (4.33) can be rewritten as:

$$\dot{Z}(t) = A_E Z(t) + B_E(P(t) + S(t)) \tag{4.41}$$

$$\dot{\Xi}(t) = C_E Z(t) \tag{4.42}$$

where $S(t) = G_{me}P_{dr}(t)$. A_E, B_E and C_E are respectively $2N \times 2N$, $2N \times N$ and $N \times 2N$ matrices of the form:

$$A_E = \begin{bmatrix} A_1 & & \\ & \ddots & \\ & & A_N \end{bmatrix}, B_E = \begin{bmatrix} B_1 & & \\ & \ddots & \\ & & B_N \end{bmatrix}, C_E = \begin{bmatrix} C_1 & & \\ & \ddots & \\ & & C_N \end{bmatrix} \tag{4.43}$$

where:

$$A_1 = \begin{bmatrix} -\gamma_{ow} & -\omega_{ow} \\ 1 & 0 \end{bmatrix},\ A_N = 0,\ A_i = \begin{bmatrix} -\gamma_{bm}(x_i) & -\omega_{bm}(x_i) \\ 1 & 0 \end{bmatrix} \tag{4.44}$$

$$B_1 = \begin{bmatrix} \frac{1}{\sigma_{ow}} \\ 0 \end{bmatrix},\ B_N = 0,\ B_i = \begin{bmatrix} \frac{1}{\sigma_{bm}} \\ 0 \end{bmatrix},\ C_i = \begin{bmatrix} 1 & 0 \end{bmatrix} \tag{4.45}$$

For $i = 2, ..., N-1$. As F is an invertible matrix, we can rewrite equation Eq. (4.39) as follows:

$$P(t) = F^{-1}\ddot{\Xi}(t) = F^{-1}C_E\dot{Z}(t) \tag{4.46}$$

It is then possible to substitute the above equation into eqaution Eq. (4.41) and obtain:

$$\dot{Z}(t) = A_E Z(t) + B_E((F^{-1}C_E\dot{Z}(t)) + S(t)) \tag{4.47}$$

$$(I - B_E F^{-1}C_E)\dot{Z} = A_E Z(t) + B_E S(t) \tag{4.48}$$

We can therefore obtain the overall state-space equation of the system:

$$M\dot{Z} = A_E Z(t) + B_E S(t) \tag{4.49}$$

$$M = (I - B_E F^{-1}C_E) \tag{4.50}$$

where M is the mass matrix of the system, which in the first formulation is linear. My Matlab implementation of the linear model can be found in the "MatlabCodes" folder under the name "lin_cochlear_model_Cecilia_Casarini".
In [1] and [26] three different implementations of the active nonlinear mechanism are outlined. I decided to insert in my code the feed-forward model proposed in [1] but using the nonlinear parameter that can be found in [6].
The pressure applied by the outer hair cells on the basilar membrane can be considered to be proportional to the total pressure of the basilar membrane, furthermore this amplification is applied to a point slightly shifted in the basilar membrane:

$$q(x + \Delta, t) = \alpha(\xi, x, t)p_{BM} = \alpha(\xi, x, t)p(x, t) + q(x, t)) \tag{4.51}$$

where q is the pressure of the outer hair cells, p_{BM} is the pressure on the basilar membrane and α is the nonlinear parameter. In my model I used the expression for α that can be found in [6] instead of that proposed in [1], as the second one did not give satisfying results regarding the saturation of the amplification, since it will be showed in the next chaper. α is therefore described by:

$$\alpha(x,\xi,t) = \alpha_0 \left[1 - tanh\left(\frac{1}{\sqrt{\lambda\pi}} \int_0^L e^{-(x-x')^2/\lambda} \frac{\xi^2(x',t)}{\xi_{sat}^2} dx'\right)\right] \tag{4.52}$$

where ξ_{sat} is tuned in order to keep the displacement ξ between 0 and 1 for stimuli in the range 40dB to 90dB. In this way the tanh function, because of its "s shape", will achieve the compressive nonlinearity and saturation as performed by the inner ear active mechanism [30].
Equation Eq. (4.51) can be rewritten as:

$$q(x,t) = \alpha(x-\Delta,\xi,t)(p(x-\Delta,t) + q(x-\Delta,t)) \tag{4.53}$$

which in the discrete approximation becomes:

$$q(x_i,t) - \alpha(x_{i-K},\xi,t)q(x_{i-K},t) = \alpha(x_{i-K},\xi,t)p(x_{i-K},t) \tag{4.54}$$

where K is an integer number and in my code it has been chosen as $K = 1$.
We can now rewrite equation Eq. (4.54) in matrix form:

$$BQ(t) = CP(t) \tag{4.55}$$

where B's diagonal is filled with 1s and, for $i = 2, ..., N-K$ its off-diagonal elements are:

$$B(i+K,i) = -\alpha(x_i,\xi,t) \tag{4.56}$$

C nonzero elements are, for $i = 2, ..., N-K$

$$C(i+K,i) = \alpha(x_i,\xi,t) \text{for } i = 2, ..., N-K \tag{4.57}$$

hence, the mass matrix of the nonlinear model is given by:

$$M = (I - B_E G(Z) F^{-1} C_E) \tag{4.58}$$

$$\text{where } G(Z) = B^{-1}C + I \tag{4.59}$$

In [1], [26] and [27] other nonlinear implementations are outlined, such as the feed-forward model (where the outer hair cells gain is proportional to the velocity of the basilar membrane) and a diagonal variation. I obtained good results with the model

described above and its Matlab implementation can be found in Appendix A.

Chapter 5

Simulations

In this chapter I will present the main results and simulations that I obtained by implementing with Matlab the Moleti model presented in [1], [26], [28], [29].
The Matlab codes used to built the model and to obtain the simulations can be found in the folder "MatlabCodes", where "lin_cochlear_model_Cecilia_Casarini" is linear, "nl_cochlear_model_Cecilia_Casarini" is nonlinear, "TEOAEs_model_Cecilia_Casarini" simulates TEOAEs and "DPOAEs_model_Cecilia_Casarini" simulates DPOAEs.
The first simulation that I obtained shows that the tonotopy is respected in the model, as one can see in Figure 5.1a, 5.1b and 5.1c. I used the linear version of the model to run these first simulations, as the tonotopy does not change in the nonlinear model and the linear implementation is faster. It can be seen that for low input frequencies, as for example 250 Hz in Figure 5.1a, the peak of the basilar membrane displacement is apical, i.e. towards the end of the basilar membrane, while for higher frequencies, as in Figure 5.1b and Figure 5.1c, the peak is basal, i.e. towards the beginning of the basilar membrane. A video showing the displacement of the basilar membrane in time with 2000 partitions and a frequency of 2000 Hz can be found in the folder attached to the digital copy (BMdisplacement_N_2000_f_2000.avi).

Another important simulation that I obtained with my Matlab code shows the difference between the linear model, i.e. when $\alpha = 0$, and the nonlinear model, in this example when $\alpha = 0.75$. As can be read in [30] the active mechanism of the outer hair cells is nonlinear and compressive; in particular this mechanism is linear between 10 dB and 30 dB, compressive between 40 dB and 90 dB and linear again for input waves of amplitude greater than 90 dB. Graphs of this kind can be often found in the literature and during my simulations I could not obtain such a result using the expression of α suggested in [1], but it was possible to eventually achieve the saturation with the one outlined in [6], as reported in Chapter 4.

After proving the nonlinear active mechanism I eventually simulated otoacoustic

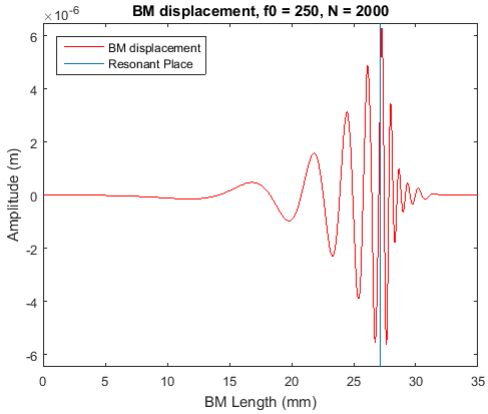

(a)

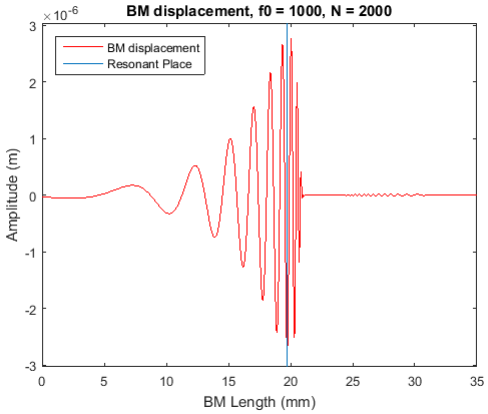

(b)

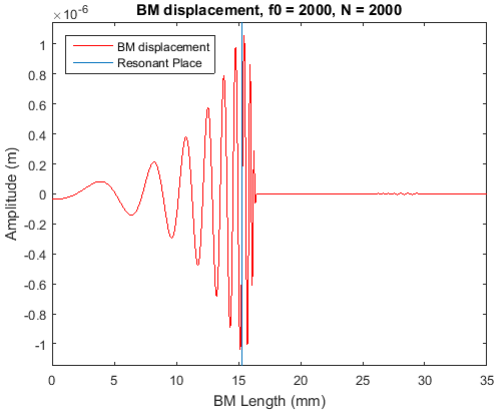

(c)

Figure 5.1: Basilar membrane displacement (Number of partitions N=2000). In the top left figure the input frequency is f=250 Hz, in the top right figure f=1000 Hz and in the bottom left figure f=2000 Hz. It can be noticed that the predicted resonant places correspond to the peak of the basilar membrane displacement and that higher frequencies have their resonant place in a basal region and lower frequencies in the apical region.

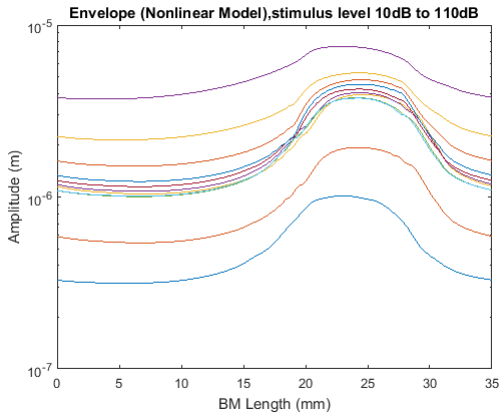

(a)

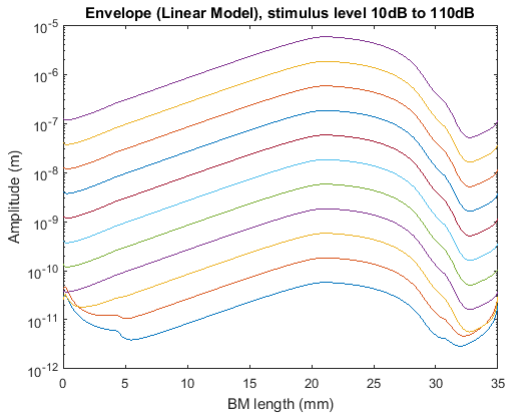

(b)

Figure 5.2: In Figure 5.2a on the left it can be seen that when alpha is nonzero there is a compression in the active mechanism for pressure waves in the range 40 dB to 90 dB. In Figure 5.2b on the right for $\alpha = 0$ the active mechanism is instead linear.

emissions, in particular I modelled TEOAEs and DPOAEs. As suggested by Moleti in [1], in order to model the emissions it is useful to add randomly distributed irregularities (represented by a roughness parameter in the code). In Figure 5.3 we can see how, when the roughness parameter is 0 (5.3b), the plot of the displacement of the stapes in time shows just the initial spike given by the evoking stimulus. Instead, when the roughness is 0.6 (5.3a), the the emission is clearly visible.

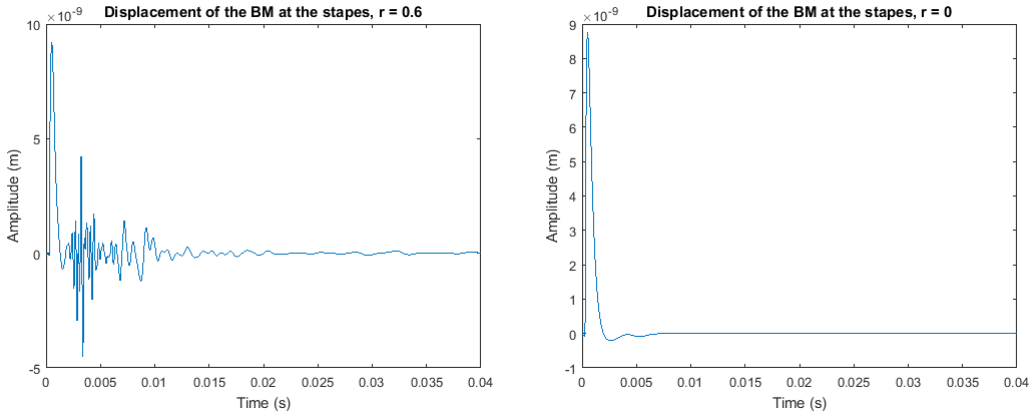

(a) (b)

Figure 5.3: Displacement of the stapes in time (N = 2). In Figure 5.3a (on the left) it can be seen that, when the roughness parameter is nonzero, the stapes have a second displacement representing the emissions after the first spike representing the stimulus. When the roughness parameter is 0 (Figure 5.3b) just the stimulus is present in the plot.

To simulate DPOAEs I used as input two sound waves with a frequency ratio of 1.22. In the simulations plotted in Figure 6.3 the stimulus frequencies are $f_1 = 2000$ Hz and $f_2 = 2440$ Hz. The amplitude of the stimuli is 80 dB, which is the one generally used in lab experiments.

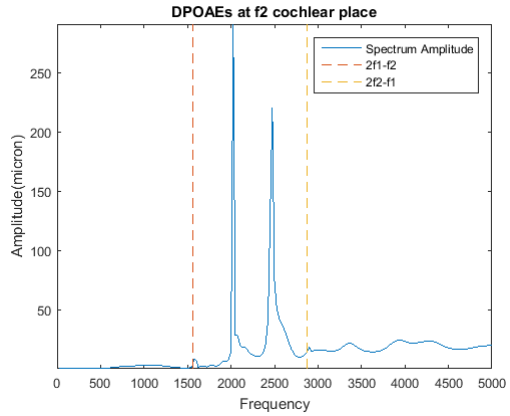

(a)

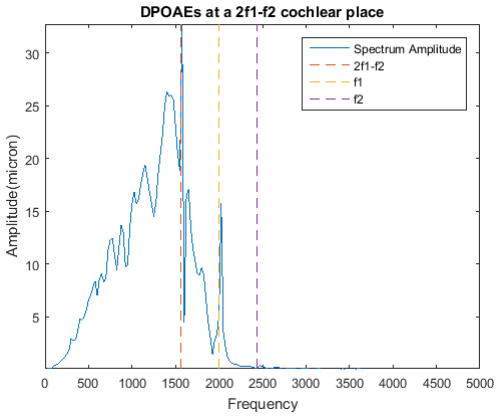

(b)

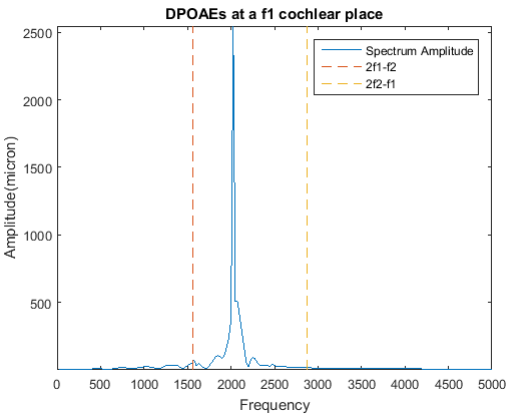

(c)

Figure 5.4: Spectrum of the signal in respectively f_2, $2f_1 - f_2$ and f_1 cochlear places. In (a) the emissions $2f_1 - f_2$ and $2f_2 - f_1$ can be clearly seen in symmetrical positions on the left and right sides of the two stimuli. In (b) $2f_1 - f_2$ has a big amplitude and f_1 can still be seen and in (c) f_1 is the highest spike and $2f_1 - f_2$ can be seen (as it is the closest).

Chapter 6

Measurements

In this chapter I will describe the results of the experimental measurements of otoacoustic emissions obtained in the lab. The experiments had the only purpose of comparing the simulations obtained in the model with some experimental measurements. Therefore, for this reason and because of the limited availability of the equipment only one subject has been tested. The specific OAEs equipment consisted of a probe (Etymotic, model ER10-C, see Figure 6.1b), containing two speakers and a microphone to be sealed in the ear, and a preamp. While the probe usually comes with a hardware and a software, we decided to purchase only the probe and the preamp and to use a NI hardware (see Figure 6.1a) and a Labview code in order to be able to better follow and be aware of every passage of the experiment. To match the different impedances of the hardware and the probes, we used a portable headphone amplifier (OPPO HA-2). All the experiments have been conducted in the anechoic chamber at the University of Edinburgh.

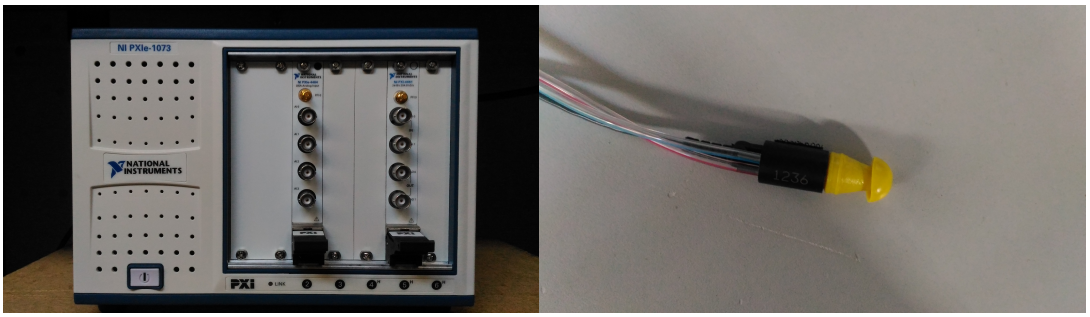

(a) National Instruments Hardware used to connect the Labview code with the probe.

(b) Etymotic ER 10-C probe.

In the first measurement I tried to obtain TEOAEs by using as stimulus a chirp in the range 100 Hz to 25000 Hz. The spectrum of the signal recorded in the ear canal is illustrated in Figure 6.2a. The interpretation of the results is not straightforward, but it can be noticed that the amplitude and the number of high frequencies are bigger than

the amplitude and the number of low frequencies: this is expected as low frequencies have a longer roundtrip from the apex to the ear canal and therefore their amplitude decays sooner. A better analysis technique and more measurements are anyway needed in order to derive reliable conclusions.

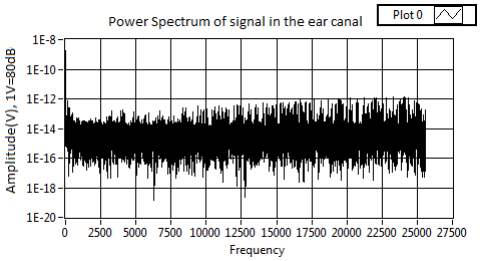

(a)

Figure 6.2: TEOAEs obtained with a chirp stimulus in the range 100 Hz to 25000 Hz.

A much more satisfying result has been obtained by measuring DPOAEs: the probe was sealed in my left ear while standing in the anechoic chamber. The input used was a 80 dB stimulus composed of two frequencies with the ratio $\frac{f_1}{f_2} = 1.22$, with f_1 taking the values 2000, 3000, 4000, 5000, 6000, 7000, 8000, 16000 and 17000 Hz. In the frequency range 2000 to 8000 Hz the emissions were evident as shown in Figure 6.3. Above all the most important DPOAEs $2f_1 - f2$ and $2f_2 - f_1$ (generally used for ear health check) were always present. In Figure 6.4 a comparison between the measured and simulated DPOAEs has been illustrated, confirming the efficiency of the physical model of the cochlea described in Chapter 4.

Finally I measured the emissions in a frequency range close to the threshold, namely $f_1 = 16000$ Hz and $f_1 = 17000$ Hz. As illustrated in Figure 6.5 the emissions are not present, even if I could still hear the input sound (the two spikes are the recordings of the initial stimulus). This is an interesting result, as when the ear is damaged, the spectrum of the recorded signal looks like the one in Figure 6.5. If a test subject has a damaged basilar membrane region or hair cells region, the input could still be heard, however the absence of the emission may be useful in order to predict a hearing loss in that frequency region in the near future. This prediction cannot be made with the same detail using an audiogram, as the test subject would still hear in that frequency range, and this is one of the reasons why studying these emissions is so important for hearing research.

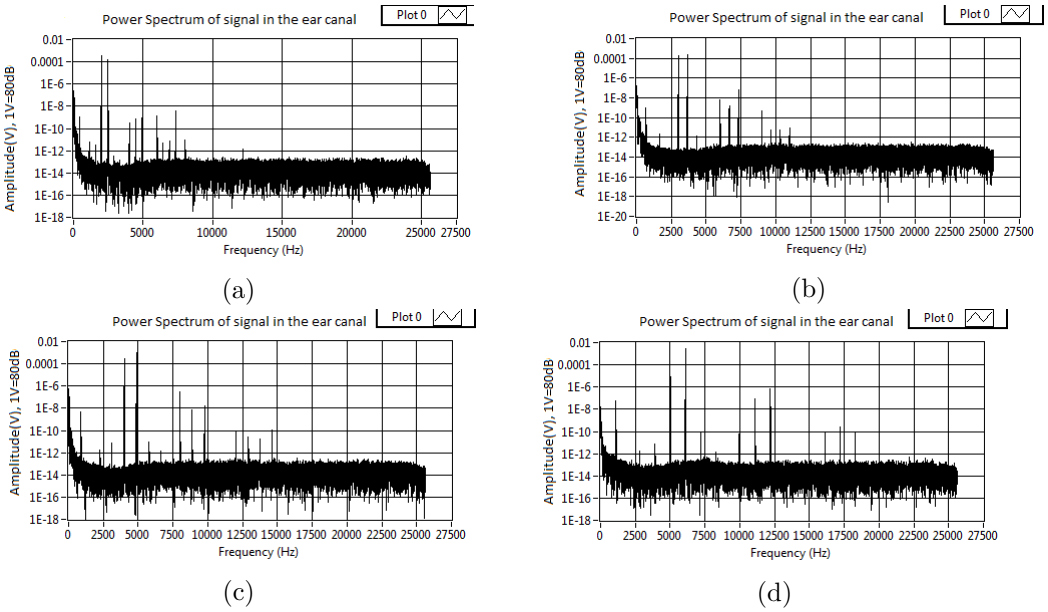

Figure 6.3: Spectrum of the signal recorded in the ear canal after playing back a 80 dB stimulus with increasing frequency f_1 and $f_2 = f_1 * 1.22$. In Figure (a) $f_1 = 2000$ Hz, in figure (b) $f_1 = 3000$ Hz, in figure (c) $f_1 = 4000$ Hz and in figure (d) $f_1 = 5000$ Hz

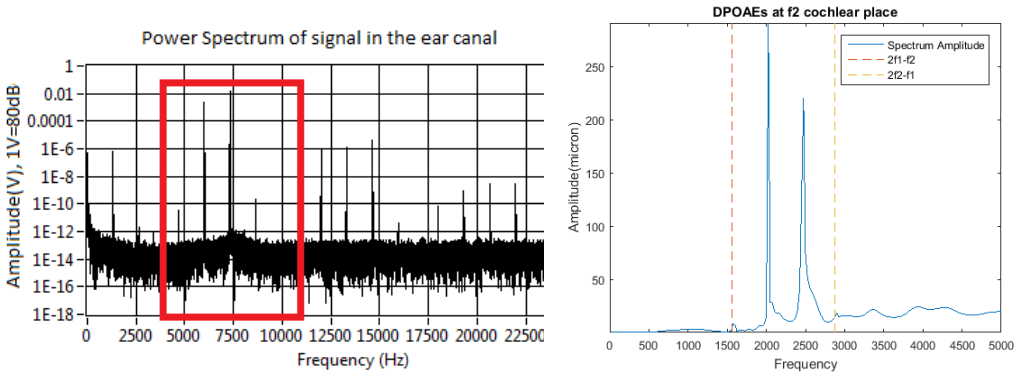

Figure 6.4: Comparison between the spectra of measured and simulated DPOAEs.

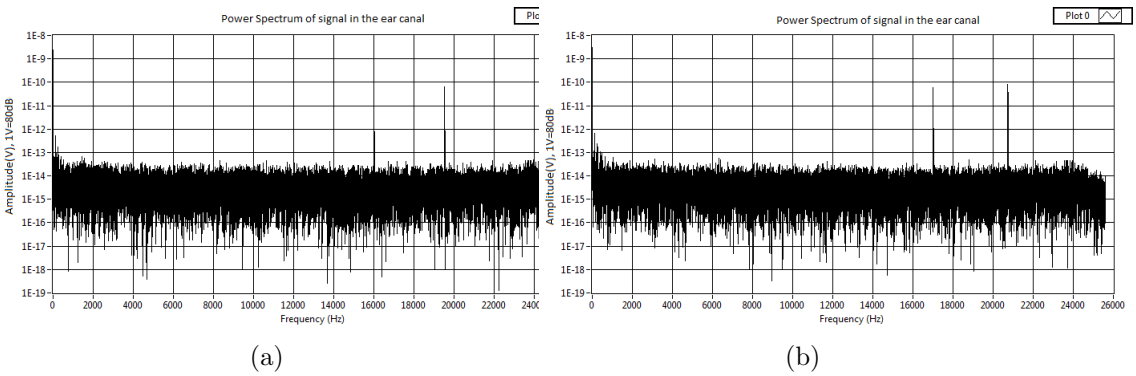

Figure 6.5: Absence of emissions in the frequency range close to the threshold.

Chapter 7

Conclusions

In my final project I have implemented, in Matlab, a physical model of the cochlea that also simulates otoacoustic emissions and I have compared these results with the measurements of OAEs conducted in the lab through a special equipment. In this dissertation I have first outlined the most important physical and physiological characteristics of the human ear and described the phenomenon of otoacoustic emissions. Subsequently, I have described the cochlear models that inspired my Matlab implementations and then I have presented the results of the simulations and I have compared them with the OAEs measurements conducted in the anechoic chamber.
In my final project proposal I initially set the goal of building a cheap software for the analysis of the emissions, preferably a phone app. Since the equipment arrived just in the last days of the project, I focused on the Matlab implementation of the cochlear model and I was able to conduct a limited amount of experiments. The results and the amount of knowledge acquired were nevertheless stimulating and represent a good and advantageous starting point for a deep research in the hearing and auditory area which I want to pursue in the future. Furthermore, the Labview code used to measure the emissions represents a first step in order to built a portable and cheap insturment for research use. The model, inspired by a paper of Moleti [1], resulted to be strong both in its linear and nonlinear formulation. The emissions were successfully simulated by adding a roughness parameter that represented the randomly distributed irregularities along the cochlea. One element of discussion about the model is represented by the fact that the distinction outlined by Shera in [4] between the emissions generated by a linear reflection and the ones that are byproduct of a nonlinear distortion is not completely clear in the model. In fact both emissions seem to be generated by the contribution of the two mechanisms. Moreover, a potential extension of the model would be the possibility of simulating SOAEs, which are not included in this implementation. A final remark is that the Matlab code required high computational times, as it took on average 6 hours to run the nonlinear version with N = 2000 and f = 2000: this is probably due to the ode45 solver, that could be substituted by a FDTD or ideally by

an analytical solution.
The experiments conducted where satisfying for what concerns DPOAEs, but a better analysis technique needs to be studied in order to measure also TEOAEs and SOAEs. In the future it would be interesting to conduct experiments on a higher number of subjects in order to be able to work on a reliable amount of data. An open question arisen from the experiments regards the possibility of substituting audiograms with OAEs screening tests in the future, not only for newborns but for adults screening as well. Finally the possibility of working with a high number of participants would be an opportunity to investigate the possibility of using OAEs as a biometric in the future, as suggested in [12], [31], [32] and [13].

Appendix A

Matlab Code

A.1 Nonlinear Model

In this appendix section the Matlab code of the nonlinear model is reported. It can be found in the "MatlabCodes" folder as "nl_cochlear_model_Cecilia_Casarini.m".

```
function nl_cochlear_model_Cecilia_Casarini()

%%%%%%%%%%%%%%%%%%%%%%%%%%%%%%%%%%%%%%%%%%%%%%%%%%%%%%%%%%%%%%%%%%%%%%%%%%%%
% This Matlab function represents a physical model of the cochlea inspired
% by the work of A.Moleti(2009). This model is nonlinear, but it can be
% turned into a linear model when alpha0=0.
% The time required to run the code grows with N, with frequency and with duration,
% therefore it is convenient to start with low N values (e.g. N=100) to
% have a first understanding of the model. Reliable results are
% nevertheless obtained with higher values (N=1000).
% The user is supposed to choose the number of cochlear partitions N,
% the duration of the simulation tEnd, the
% input frequency f0 and the amplitude of the signal a in dB (that will be
% converted automatically in Pascals).
% The plot generated represents the basilar membrane displacement in a
% steady moment towards the end of the simulation.
% The matrix Y is saved by the code and it will contain the displacement in
% its even columns and the velocity of the BM in its odd columns. The lines
% represent the time of the simulation.
%%%%%%%%%%%%%%%%%%%%%%%%%%%%%%%%%%%%%%%%%%%%%%%%%%%%%%%%%%%%%%%%%%%%%%%%%%%%

close all
clc

% Start of time measurement of the code
tic;

%%%%%%%%%%%%%%%%%%%% MECHANICAL AND PHYSICAL PARAMETERS %%%%%%%%%%%%%%%%%%%%
```

```
29
30 % Timing of the simulation (s)
31 tEnd = 0.02;
32
33 % Input Frequency (Hz)
34 f0 = 500;
35
36 %Number of Micromechanical Elements +2 boundary conditions
37 N = 100;
38
39 % Amplitude in dB
40 adB = 80;
41
42 % Convertion to Pascals
43 aPa = 10^(adB/20)*0.00002;
44
45 % Time vector to be given to the ode45 solver
46 tspan = [0,tEnd];
47
48 % Length of the BM (m)
49 L = 3.5*(10^(-2));
50
51 % Fluid density (Kg*m^(-3))
52 rho = 10^3;
53
54 % Lenght of each cochlear partition (m)
55 delta = L/(N-2);
56
57 % Height (m)
58 H = 0.001;
59
60 % Greenwood map frequency coefficient (s^(-1))
61 omega0 = 2.0655*(10^4)*2*pi;
62
63 % Greenwood map inverse length scale (m^(-1))
64 k_w = 1.382*(10^2);
65
66 % Effective middle ear - oval window damping (S^(-1))
67 gamma_ow = 5*(10^3);
68
69 % Effective middle ear - oval window density (Kg*m^(-2))
70 sigma_ow = 2;
71
72 % BM density (Kg*m^8-2))
73 sigma_bm = 5.5*(10^(-2));
74
75 % Effective middle ear-oval window stiffness ( N*m^(-3))
76 K_ow = 2*(10^8);
77
```

```
% Middle ear frequency
omega_ow = sqrt(K_ow/sigma_ow); % = 10000

% middle ear mechanical gain of the ossicles
G_me = 21.4;

% OHC non-local interaction range (squared) (m^2)
lambda = 1.2*10^(-7);

% Integer number to be used in the nonlinear mass matrix
K = 1;

% Greenwood equations:

% 1) Place-frequency map
omega_bm = omega0 * exp(-k_w * ((1:(N-2))*delta));

% Expected cochlear place
position = (-(log((f0*2*pi)/omega0))/(k_w))*(N-2)/L;
position = round(position);

% 2) Passive linear damping
% Tuning parameter
Q = 8;
gamma_bm = omega_bm/Q;


%%%%%%%%%%%%%%%%%%%%%%%%%% MATRICES CALCULATION %%%%%%%%%%%%%%%%%%%%%%%%%%

% F Matrix
F = zeros(N,N);
F(1,1) = -delta/H;
F(1,2) = delta/H;
F(N,N) = -2*rho*(delta^2)/H;

i=1;
for j=2:N-1
    F(j,i)= 1;
    F(j, i+1) = -2;
    F(j, i+2) = 1;
    i = i+1;
end

F = H/((2*rho)*(delta^2))*F;
F = sparse(F); % keeps only the non-zero components (to speed up the code)

% A matrix
A = cell(1, N);
A{1} = [-gamma_ow,-(omega_ow)^2; 1, 0];
```

```
127 A{N} = [0, 0; 0, 0];
128
129 for n = 2:N-1
130     A{n} = [-gamma_bm(n-1),-(omega_bm(n-1))^2; 1, 0];
131 end
132
133 % Ae matrix
134 Ae = blkdiag(A{1:N});
135 Ae = sparse(Ae);
136
137 % B matrix
138 B = cell(1,N);
139
140 B{1} = [1/sigma_ow; 0];
141 B{N} = [0;0];
142
143 for n = 2:N-1
144     B{n} = [1/sigma_bm; 0];
145 end
146
147
148 % Be matrix
149 Be = blkdiag(B{1:N});
150 Be = sparse(Be);
151 % C matrices
152 C = cell(1,N);
153
154 for n = 1:N
155     C{n} = [1,0];
156 end
157
158 % Ce matrix
159
160 Ce = blkdiag(C{1:N});
161 Ce = sparse(Ce);
162
163 % I
164 I = eye(2*N);
165 I = sparse(I);
166
167 % S(t)
168 S = zeros(N,1);
169 S(1,1) = G_me;
170 S = sparse(S);
171
172 %%%%%%%%%%%%%%%%%%%%%%%%%%%% ODE SOLVER %%%%%%%%%%%%%%%%%%%%%%%%%%%%
173 initial_conditions = zeros(2*N,1);
174 options = odeset('mass', @Mnonlin_func);
175
```

```
[T,Y]=ode45(@DoubleDOF_1stOrderSystem,tspan,initial_conditions,options);
size(Y)

% %%%%%%%%%%%%%%%%%%%%%%%%%%%% SIMULATION %%%%%%%%%%%%%%%%%%%%%%%%%%%%%%%%%%%%
% x axis for the plot
x = linspace(0,L,N-2);

% Matrix containing the BM displacement in time
y_displacement = Y(1:size(Y,1), 4:2:2*N-2);

% Matrix containing the BM velocity in time
y_velocity = Y(1:size(Y,1), 3:2:2*N-3);

[Maxvalue, Index] = max(max(y_displacement));
plot(x,y_displacement(size(y_displacement,1)-2,:),'r',Index*L/(N-2)*ones(1,100),...
    linspace(min(min(y_displacement)), max(max(y_displacement)),100),'c');
axis([0 L min(min(y_displacement)) max(max(y_displacement))])
xlabel('BM length (m)');
ylabel('Amplitude (m)');
title('BM DISPLACEMENT');
legend('BM displacement', 'Resonant place','Location','northwest');


%%%%%%%%%%%%%%%%%%%%%%%%%%%%%%%% MAIN FUNCTIONS %%%%%%%%%%%%%%%%%%%%%%%%%%%%%%%%

% Nested function that sets up the 1st order system to be used by ODE solver
    function Zdot = DoubleDOF_1stOrderSystem(t,Z)

        %%%%%%%%%%%%%%%% Main state space system equation %%%%%%%%%%%%%%%
        Zdot = Ae*Z + Be*(S*(aPa*cos(2*pi*f0*t)));

    end

% Nested function representing the mass matrix of the system. When alpha0 =
% 0 the mass matrix is linear.
    function Mnonlin = Mnonlin_func(t,Z)

        alpha = zeros(1,N);
        Bnl=zeros(N,N);
        sat = 10^(-5); % parameter to be tuned to achive the saturation
        alpha0 = 0.75;
        for r=2:N-1
            dummy = 0;
            for s = 2:N-1


                % This is the version of alpha as suggested by Botti (2009)
                % 1)
                alphatemp =  (1/sqrt(lambda*pi))*(((1/sat)^2)*(Z(s*2,:))^2)...
```

```
225                     * exp(-((r*delta-s*delta)^2));
226
227                 %Integration = area under function --> sum of function*delta
228                 dummy = dummy + alphatemp*delta;
229
230             end
231
232             % For big values of dummy tanh = 1 ---> alpha = 0
233             alpha(r) = alpha0 * (1-tanh(dummy));
234
235         end
236
237
238         % Matrices for the nonlinear Mass function
239         for o = 2:N-1-K
240             Bnl(o+K,o)=-alpha(o);
241         end
242
243         Bnl(N,N)=0;
244         Bnl = Bnl + eye(N);
245         Cnl = -Bnl + eye(N);
246
247         % Mass functions as suggested by Moleti(2009) - Feedforward
248         % approximation
249
250         G = inv(Bnl)*Cnl + eye(N);
251         Mnonlin = I - ((Be*G)*inv(F))*Ce;
252         Mnonlin=sparse(Mnonlin);
253
254     end
255
256 % Saving the important parameters and matrices
257 save(sprintf('Casarini_C_nl_cochlear_model_N%d_f0%d_a%d.mat',N, f0, adB),'Y',...
258     'T', 'Index','Maxvalue', 'position','f0', 'N', 'tEnd', 'adB' );
259
260 % End of time measurement
261 toc;
262
263 end
```

A.2 Linear Model

As explained in the comments of the code in the previous section, it is possible to obtain a linear model (i.e. representing the 'dead cochlea') by assigning the value 0 to the parameter α. However the "MatlabCodes" folder will also contain a linear model code named "lin_cochlear_model_Cecilia_Casarini.m", where the mass matrix (line 211 to 235 in the code printed above) has been directly changed to:

```
function Mlin = Mlin_func(t,Z)

        Mlin = I - Be*inv(F)*Ce;

end
```

A.3 TEOAEs

The code for the simulation of the TEOAEs can be found in the MatlabCodes folder under the name "TEOAEs_Cecilia_Casarini.m". It is a modification of the nonlinear code in the following way:

- The input is represented by a sinc function; therefore, there is no need to choose f0;
- The state space equation is changed in:

```
%%% Main state space system equation %%%%
Zdot = Ae*Z + Be*(S*aPa*(sinc((t-0.0002)/0.0002)));
```

- The roughness parameter is inserted in the model:

```
% Roughness parameter
roughness = 0.6;
for n = 2:N-1
    A{n} = [-gamma_bm(n-1),(-(omega_bm(n-1))^2)*...
    (1+roughness*(rand(1)-0.5)); 1, 0];
end
```

- The plot is obtained by:

```
% Plot of the displacement of the base in time. It can be seen that when
% roughness is different from 0 there is a second wave moving the stapes
% after the stimulus.
x = linspace(0,tEnd,size(Y,1));
plot(x,Y(:,2));
title('Stapes displacement in time');
xlabel('Time (s)')
ylabel('Amplitude (m)')
```

A.4 DPOAEs

The code for the simulation of the DPOAEs can be found in the MatlabCodes folder under the name "DPOAEs_Cecilia_Casarini.m". It is a modification of the nonlinear code in the following way:

- The input is represented by two frequencies with the ratio 1.22

```
% Input Frequencies (Hz)
f0 = 2000;
f1 = f0*1.22;
fdp = 2*f0-f1;
```

- The state space equation is changed in:

```
%%%%%%%%%%%%%%% Main state space system equation %%%%%%%%%%%%%%%
        Zdot = Ae*Z + Be*(S*(aPa*(sin(2*pi*f0*t)+sin(2*pi*f1*t))));
```

- The roughness parameter is inserted in the model:

```
% Roughness parameter
roughness = 0.6;
for n = 2:N-1
    A{n} = [-gamma_bm(n-1),(-(omega_bm(n-1))^2)*...
    (1+roughness*(rand(1)-0.5)); 1, 0];
end
```

- The plot is obtained by:

```
% Signal to analyse (choose the cochlear place)
cp = Y(:,position1*2);
% Number of samples to include in the spectrum
fft_length = size(Y,1);
P2 = abs(fft(cp)/fft_length);
P1 = P2(1:fft_length/2+1);
P1(2:end-1) = 2*P1(2:end-1);
Fs=size(Y,1)/0.02;
f = Fs*(0:(fft_length/2))/fft_length;
plot(f,P1)
title('Spectrum of the signal in f1 cochlear place')
xlabel('f (Hz)')
ylabel('Magnitude')
axis([0 5000 0 +inf])
```

Appendix B

Labview Code

In this Appendix I will briefly illustrate the Labview code used for measuring DPOAEs and TEOAEs. The codes can be found in the "LabviewCodes" folder with the names "DPOAEs_Cecilia_Casarini" and "TEOAEs_Cecilia_Casarini".

B.1 DPOAEs

Figure B.1 shows the block diagram of the Labview codes used to measure DPOAEs. Since the image is small I have divided the code in three sections, as shown in Figure B.2 and explained each section in the following page.
In Figure B.3, corresponding to the red section, the two input sinusoids are built with an express VI and the user is able to change their frequency and amplitude from the front panel. In Figure B.4, corresponding to the blue section, the physical channels for the input microphone and the output signals (played by the speakers) are chosen and connected to the physical NI hardware. Finally Figure B.5, corresponding to the green section, shows the synchronization of the input and the output: the microphone will begin to read samples and at the same moment the output channels will emit their signals. Furthermore the microphone reads an additional number of samples: in this way it is possible to record the response in the ear canal after the signal has been stopped and therefore to record transient emissions. The parts of the code outside the sections are responsible for plotting and saving the signal.

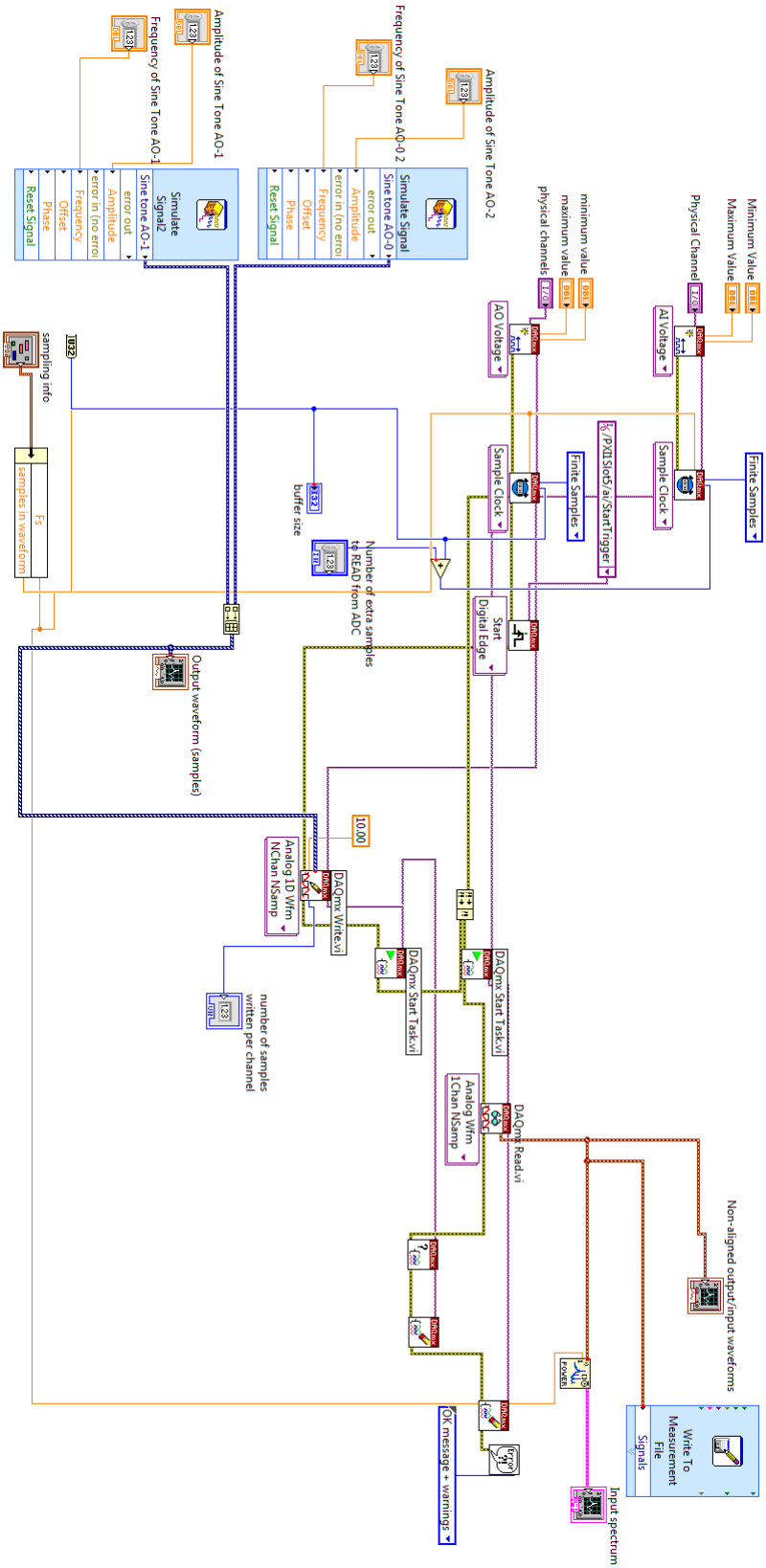

Figure B.1: DPOAEs Labview code.

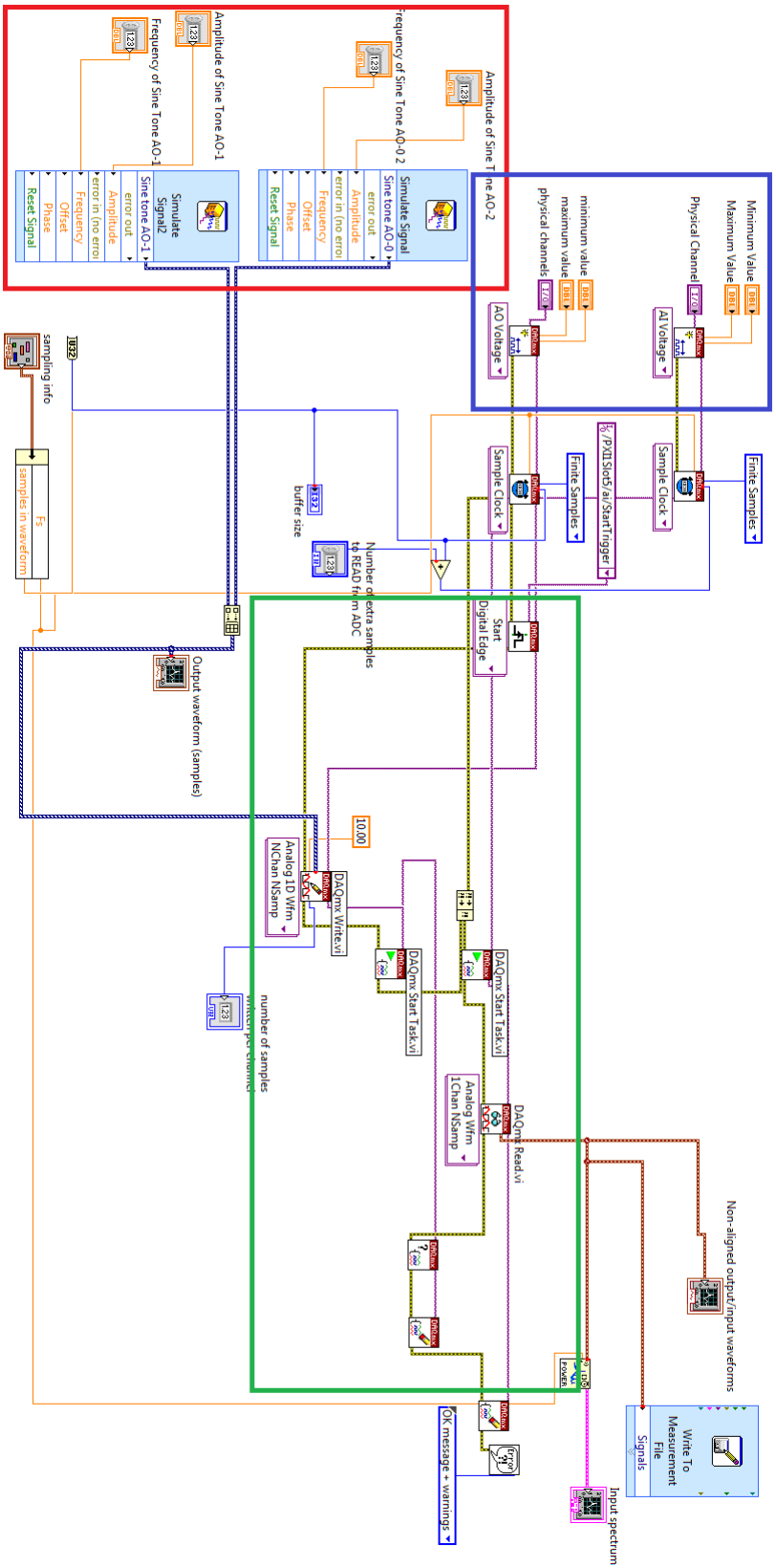

Figure B.2: DPOAEs Labview code divided in sections.

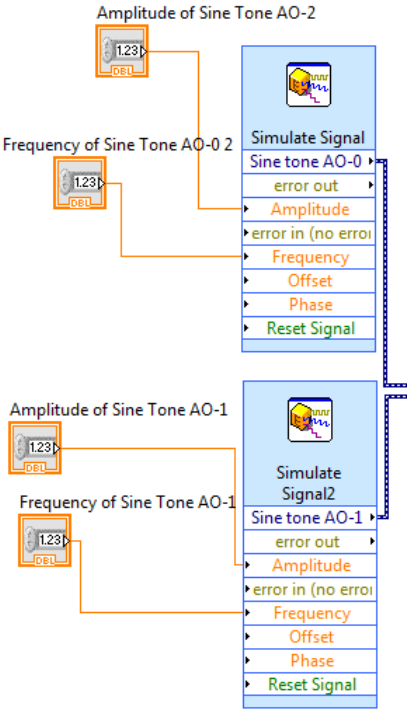

Figure B.3: Sinusoids used to evoke DPOAEs (red section).

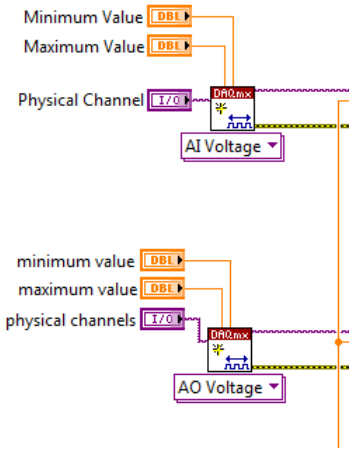

Figure B.4: Physical Channels Input/Output (blue section).

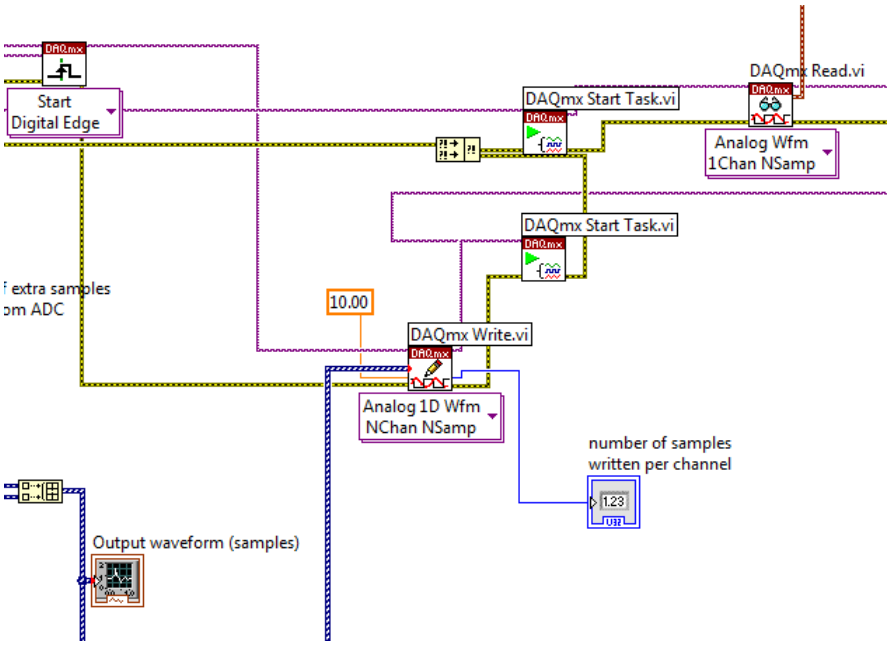

Figure B.5: Synchronization of input and output (green section).

B.2 TEOAEs

The Labview code used to measure TEOAEs is really similar to the one used to measure DPOAEs and described in the previous section. The main difference is illustrated in Figure B.6, that shows how the stimulus is a chirp signal taken from the signal processing Labview palette.

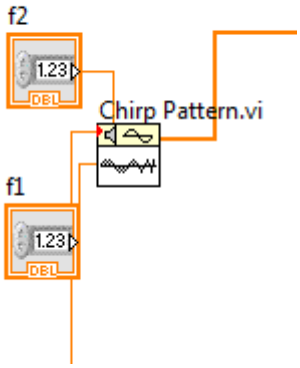

Figure B.6: Chirp signal used to evoke TEOAEs.

Bibliography

[1] A. Moleti, N. Paternoster, D. Bertaccini, R. Sisto, and F. Sanjust, "Otoacoustic emissions in time-domain solutions of nonlinear non-local cochlear models," *J. Acoust. Soc. Am., Vol. 126, No. 5*, 2009.

[2] J. O. Pickles, *An Introduction to the Physiology of Hearing.* Emerald, 2008.

[3] J. Siegel, "Otoacoustic emissions," *Allan I., Basbaum, Akimichi Kaneko, Gordon M. Shepherd and Gerald Westheimer, editors The Senses: A Comprehensive Reference, Vol 3, Audution, Peter Dallos and Donata Oertel. San Diego: Academic Press; p. 237–262*, 2008.

[4] C. Shera and J. J. Guinan Jr., "Evoked otoacoustic emissions arise by two fundamentally different mechanisms: A taxonomy for mammalian oaes," *J. Acoust. Soc. Am. 105(2), 782-798*, 1999.

[5] S. Neely and D. Kim, "A model for active elements in cochlear biomechanics," *J. Acoust. Soc. Am. 79 (5), 1472-1480*, 1986.

[6] T. Botti, "Risposta evocata da stimoli acustici in modelli cocleari attivi nonlineari e nonlocali, risolti numericamente nel dominio del tempo," Master's thesis, University of Tor Vergata (Rome), 2009.

[7] T. Reichenbach and J. Hudspeth, "The physics of hearing: fluid mechanics and the active process of the inner ear," *Rep. Prog. Phys. 77 076601 (45pp)*, 2014.

[8] T. Gold, "Hearing. ii. the physical basis of the action of the cochlea," *Proc. R. Soc. Lond. B. Biol. Sci., 135:492–498*, 1948.

[9] D. T. Kemp, "Stimulated acoustic emissions from within the human auditory system," *J. Acoust. Soc. Am. 64, 1386–1391*, 1978.

[10] T. Van De Water, A. Popper, and R. R. Fay, *Clinical Aspects of Hearing.* Springer, 1996.

[11] *Concepts and Challenges in the Biophysics of Hearing*, 2008.

[12] M. Swabey, S. P. Beeby, A. D. Brown, and J. Chad, "Using otoacoustic emissions as a biometric," *School of Electronics and Computer Science, University of Southampton (UK)*, 2004.

[13] J. F. Gao, D. Agrafioti, S. Wang, and D. Hatzinakos, "Transient otoacoustic emissions for biometric recognition," *IEEE International Conference on Acoustics, Speech and Signal*, 2012.

[14] D. Kemp and R. Chum, "Properties of the generator of stimulated acoustic emissions," *Hear. Res., 2, 213-232.*, 1980.

[15] D. T. Kemp, "Otoacoustic emissions in perspective," *Otoacoustic Emissions: Clinical Applications, edited by M. S. Robinette and T. J. Glattke (Thieme, New York), pp. 1–21*, 1997.

[16] D. Kemp and A. Brown, "An integrated view of the cochlear mechanical nonlinearities observable in the ear canal," *E. de Boer & M.A. Viergever (Eds) Mechanics of Hearing (pp. 75-82). The Hague, The Netherlands: Martinus Nijhoff*, 1983.

[17] *What Fire is in Mine Ears - Progress in Auditory Biomechanics*, 2011.

[18] C. A. Shera and G. Zweig, "Noninvasive measurement of the cochlear travelling-wave ratio," *J. Acoust. Soc. Am. 93, 3333–3352*, 1993.

[19] G. von Békésy and E. Wever, *Experiments in hearing.* 1960.

[20] E. M. Ku, *Modelling the Human Cochlea.* PhD thesis, University of Southampton, Institute of Sound and Vibration Research (Faculty of Engineering, Science and Mathematics), 2008.

[21] S. J. Elliott, E. M. Ku, and B. Lineton, "A state space model for cochlear mechanics," *J. Acoust. Soc. Am. 122(5), 2759-2771*, 2007.

[22] E. de Boer, "Mechanics of the cochlea: Modeling efforts," *The cochlea, edited by P. Dallos, A. N. Popper, and R. R. Fay. Springer-Verlag, New York, 258-317*, 1996.

[23] P. Dallos, A. Popper, and F. R.R, *The Cochlea.* Springer, 1996.

[24] S. J. Elliott, B. Lineton, and N. Guanjian, "Fluid coupling in a discrete model of cochlear mechanics," *J. Acoust. Soc. Am., Vol. 130, No. 3*, 2011.

[25] S. Pan, S. J. Elliott, P. Teal, and B. Lineton, "Efficient time-domain simulation of nonlinear, state-space, transmission-line models of the cochlea (l)," *J. Acoust. Soc. Am., Vol. 137, No. 6*, 2015.

[26] R. Sisto, A. Moleti, P. N., T. Botti, and D. Bertaccini, "Different models of the active cochlea, and how to implement them in the state-space formalism," *J. Acoust. Soc. Am., Vol. 128, No. 3*, 2010.

[27] R. Sisto, F. Sanjust, and A. Moleti, "Input/output functions of different-latency components of transient-evoked and stimulus-frequency otoacoustic emissions," *J. Acoust. Soc. Am., Vol. 133, No. 4*, 2013.

[28] A. Moleti, F. Longo, and R. Sisto, "Time-frequency domain filtering of evoked otoacoustic emissions," *J. Acoust. Soc. Am., Vol. 132, No. 4*, 2012.

[29] A. Moleti, T. Botti, and R. Sisto, "Transient-evoked otoacoustic emission generators in a nonlinear cochlea," *J. Acoust. Soc. Am., Vol. 131, No. 4*, 2012.

[30] K. Lim and C. Steele, "A three-dimensional nonlinear active cochlear model analyzed by the wkb-numeric method," *Hearing Research 170 190 205*, 2002.

[31] N. J. Grabham, M. A. Swabey, P. Chambers, M. Lutman, N. White, and S. Chad, J.E. Beeby, "An evaluation of otoacoustic emissions as a biometric," *IEEE Transactions on Information Forensics and Security*, 2013.

[32] M. Swabey, S. P. Beeby, A. D. Brown, and J. Chad, "Investigation into the uniqueness of neonate transient otoacoustic emissions," *School of Electronics and Computer Science, University of Southampton (UK).*, 2004.